# Precision Measurements of the Proton Structure

*Iris Abt*[1] on behalf of the H1 and ZEUS collaborations[2]

[1]MPI für Physik, Föhringer Ring 6, 80805 München, Germany
[2]DESY, Notkestraße 85, 22607 Hamburg, Germany

**DOI:** `http://dx.doi.org/10.3204/DESY-PROC-2012-02/7`

The "proton structure" is a wide field. Discussed are predominantly the precision measurements of the proton structure functions at HERA and some of their implications for the LHC measurements. In addition, a discussion of what a proton structure function represents is provided. Finally, a connection to nuclear physics is attempted.

## 1 Introduction

The proton is quite a fantastic particle. If free, it doesn't decay on any timescale people have been able to explore. It has an immense ability to heal itself, demonstrated in the high rate of diffraction even for interactions with large momentum transfer. What the author really knows, is actually quite limited. The charge was determined to be "+1", the mass was measured to be $1.6 \times 10^{-27}$ kg and the spin is 1/2. Spin will not be discussed in this contribution; there are others who will write about it.

If the proton is probed with enough energy, three valance quarks are revealed. If it is probed with even more energy, the QCD affliction of the proton, i.e. the glue and the sea become visible. QCD is always used when the results of one measurement are used to make predictions for another. And one part of this *ansatz* are parton distributions functions, PDFs, of the proton. They are a very successful tool. However, their shape is entirely heuristic; QCD cannot predict them from first principle.

Protons are a vital part of nuclei. Together with neutrons, they provide the rich world of elements that we so dearly love. However, in this environment QCD is generally not the theory of choice to predict what happens. Inside a nucleus, a proton can decay because the energy to become a neutron comes from the nucleus. Nuclei are not spheres; the proton itself is often depicted as one, but that is also too simplistic.

## 2 Proton Structure Functions at HERA

### 2.1 Deep Inelastic Scattering

At HERA, the structure of the proton was probed with electrons and positrons. Figure 1 illustrates deep inelastic scattering, DIS, which is generally used to determine the proton structure. The castle is destroyed to learn about its inhabitants, i.e. the quarks and gluons, and their habits. It is interesting to note that the castle rebuilds itself in about 20 % of the interactions. However, this, i.e. diffraction, is not the subject of this contribution.

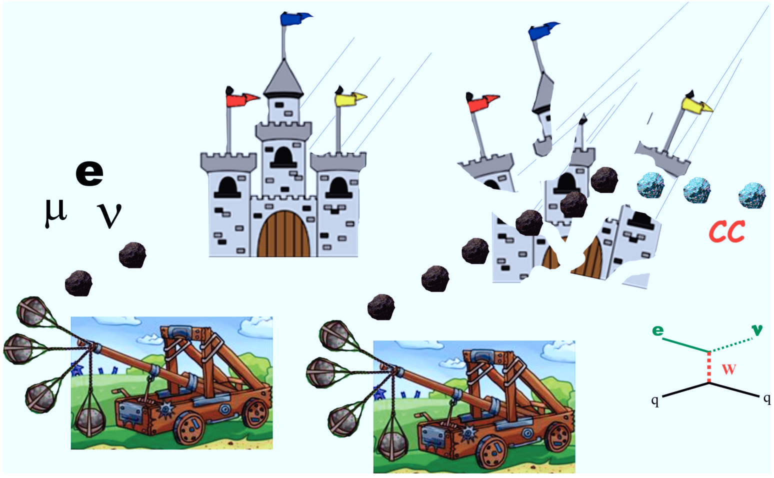


Figure 1: Illustration of deep inelastic lepton proton scattering. At HERA the lepton was an electron or positron. In this demonstration, a charged current interaction destroys the proton.

More commonly used to illustrate DIS is the Feynman diagram depicted in Figure 2. It should, however, be noted that this Feynman diagram describes the interaction in lowest order while Figure 1 includes all orders. Anyhow, the process can be described in terms of the kinematic variables $x$, $y$, and $Q^2$. The variable $Q^2$ is defined as $Q^2 = -q^2 = -(k-k')^2$, where $k$ and $k'$ are the four-momenta of the incoming and scattered lepton, respectively. Bjorken $x$ is defined as $x = Q^2/2P \cdot q$, where $P$ is the four-momentum of the incoming proton. The fraction of the lepton energy transfered to the proton in the rest frame of the proton is given by $y = P \cdot q / P \cdot k = Q^2/sx$, where $s$ is the square of the lepton-proton centre-of-mass energy.

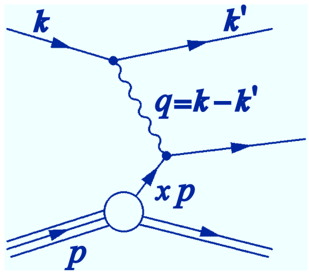


Figure 2: Feynman diagram of deep inelastic lepton proton scattering

In neutral current, NC, events, most of the information can be deduced from the deflected probe. However, quite often the hadronic system is also used in order to optimise the uncertainties. In charged current, CC, events, the outgoing neutrino evades detection and the hadronic system is all we have. This makes things are a lot more difficult.

## 2.2 Cross sections

All our understanding of DIS is connected to the paradigm of factorisation.

In lowest-order QCD, three processes contribute to the NC DIS cross section, namely the Born ($V^*q \to q$, with $V^* = \gamma^*, Z^*$), the boson-gluon-fusion ($V^*g \to \bar{q}q$) and QCD-Compton-scattering ($V^*q \to qg$) processes. The cross section for the production of an observed hadron,

$H$, in the final state in DIS can be expressed in QCD, using the factorisation theorem, as

$$\sigma(ep \to e + H + X) = \sum_{j,j'=q,\bar{q},g} f_{j/p}(x,Q) \otimes \hat{\sigma}_{jj'}(x,Q,z) \otimes F_{H/j'}(z,Q),$$

where the sum runs over all possible initial (final)-state partons $j$ ($j'$), $f_{j/p}$ are the proton PDFs, which give the probability of finding a parton $j$ with momentum fraction $x$ in the proton, $\hat{\sigma}_{jj'}$ is the partonic cross section, which includes the matrix elements for the three processes mentioned above, and $F_{H/j'}$ are the fragmentation functions, which give the probability that a hadron $H$ with momentum fraction $z$ originates from parton $j'$.

This contribution concentrates on inclusive measurements, so that the fragmentation "only" shows up in the calculation of the systematic uncertainties connected to the acceptance and the efficiency to reconstruct an event. The cross sections are measured and their description in QCD is used to extract the PDFs which in turn are used to make predictions. This works extremely well as long as the same assumptions are made for the extraction and the predictions.

For a complete overview of neutral current, NC, and charged current, CC, cross sections, please check your favorite textbook. The electroweak Born-level cross section for the $e^{\pm}p$ NC interaction serves as an example here:

$$\frac{d^2\sigma(e^{\pm}p)}{dxdQ^2} = \frac{2\pi\alpha^2}{xQ^4}[Y_+\tilde{F}_2(x,Q^2) \mp Y_- x\tilde{F}_3(x,Q^2) - y^2\tilde{F}_L(x,Q^2)], \quad (1)$$

where $\alpha$ is the fine-structure constant, $Y_{\pm} = 1 \pm (1-y)^2$ and $\tilde{F}_2(x,Q^2)$, $\tilde{F}_3(x,Q^2)$ and $\tilde{F}_L(x,Q^2)$ are generalised structure functions. The contribution of the longitudinal structure function $\tilde{F}_L$ to $d^2\sigma/dxdQ^2$ is approximately 1 %, averaged over the relevant kinematic range; it contributes up to 10 % at high y. The $\tilde{F}_3$ term only starts to contribute significantly at $Q^2$ values of the order of the mass of the $Z$ boson squared.

The reduced cross sections for NC $e^{\pm}p$ scattering are defined as

$$\tilde{\sigma}^{e^{\pm}p} = \frac{xQ^4}{2\pi\alpha^2}\frac{1}{Y_+}\frac{d^2\sigma(e^{\pm}p)}{dx}dQ^2 = \tilde{F}_2(x,Q^2) \mp \frac{Y_-}{Y_+}x\tilde{F}_3(x,Q^2) - \frac{y^2}{Y_+}F_L(x,Q^2). \quad (2)$$

The $x\tilde{F}_3$ can be obtained from the difference of the $e^-p$ and $e^+p$ cross section.

The different structure functions in the Born-level approximation are directly connected to different combinations of quark momentum distributions. The structure function $\tilde{F}_3$, for example, provides information about the $u$ and $d$ valence quarks.

## 2.3 The advent of precision

The definition of precision is certainly not objective and what it really means in this context is debatable. However, from the viewpoint of HERA, precision structure functions came about when the two experiments, H1 and ZEUS, started to combine their already individually beautiful data.

The two collaboration published their combined results on data taken in the period of 1993 – 2000 in 2010 [1]. The 10 years it took indicate that such a combination is difficult. The bins and the kinematic ranges need to be adjusted, the uncertainties evaluated according to their correlation, and, in order to do so, the team has to understand both experiments. The result is depicted in Fig. 3. Due to the careful analysis of the correlations between the systematic

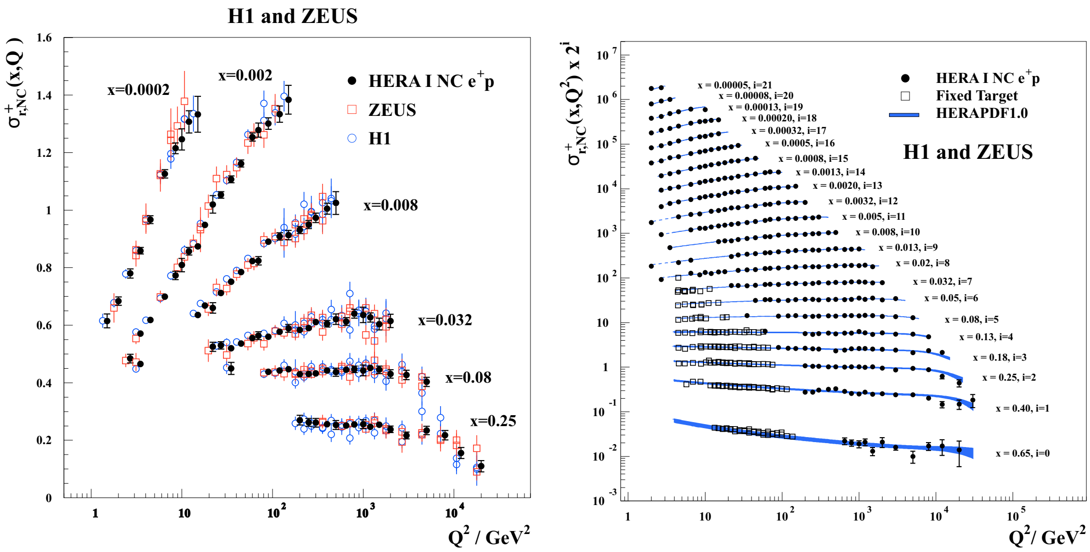


Figure 3: Combination of reduced cross section from [1]. The left panel demonstrates the power of combination for selected values of x while the right panel shows the wide kinematic range covered by HERA.

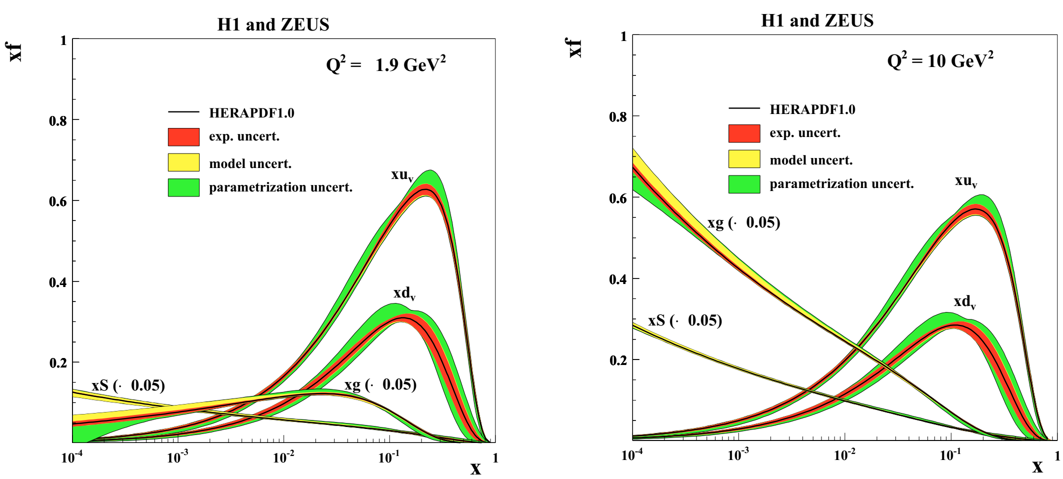


Figure 4: HERAPDF1.0: The left panel demonstrates the importance of the valence quarks at relatively low $Q^2$ while the right panel shows the growth of the sea and the glue with $Q^2$. Please note that sea and glue are scaled down by a factor 20.

uncertainties, the gain is significantly larger than expected if only the statistical precision is considered.

The results of the combination were used to produce the first HERAPDF [1], entirely deduced from HERA inclusive data, see Fig. 4.

## 2.4 The PDF fitting industry

There is quite a number of groups who perform fits to a wide variety of data sets in order to extract PDFs. They go by acronyms representing names or ideas, in alphabetic order: ABKM, CTEQ, HERAPDF, GJR, NNPDF, MSTW. The acronyms are usual augmented by a version number. HERAPDF was so far restricted to HERA data. Other groups use HERA data, but not exclusively.

Different PDFs can be extracted at varying order in perturbative QCD, using different flavor schemes, different parameters like charm mass and different parametrisations. It is of great importance to use the same schemes and assumptions used for the extraction when making a prediction. The predictions you see in the plots showing cross sections were of course all extracted keeping that in mind.

## 2.5 Towards the final HERA precision

The data taking period that will provide the final precision in cross sections and PDFs from HERA is the HERA II period from 2004 to 2007. The data are still being analysed and some results are only available as preliminary releases so far. It is expected that both the H1 and ZEUS collaborations will publish final results this summer.

Figure 5 gives a taste of the precision obtained from HERA II data. At high $Q^2$, the NC and CC cross sections become equal because the $Z^0$ starts to dominate over the photon. The difference between electron and positron data also becomes clearly visible at high $Q^2$.

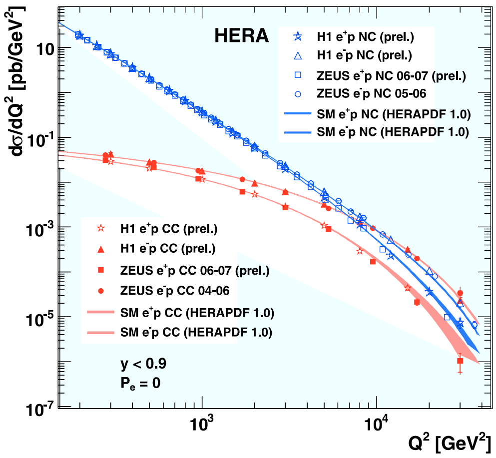


Figure 5: A demonstration how precision data reveal the unification of the electroweak force and parity violation at $Q^2 > m^2_{Z^0}$.

The CC data also provide other valuable information. As there is no interference from photon exchange, the CC process was used to check the V-A structure of the weak interaction using the polarisation of the lepton beam in HERA II [2]. However, for this contribution the access to the quark structure of the proton is more interesting. As an example, Fig. 6(left) shows the reduced cross sections for CC positron interaction as published by ZEUS [3] . These data give access to the $d$ and $s$ as well as $\bar{u}$ and $\bar{c}$ content of the proton.

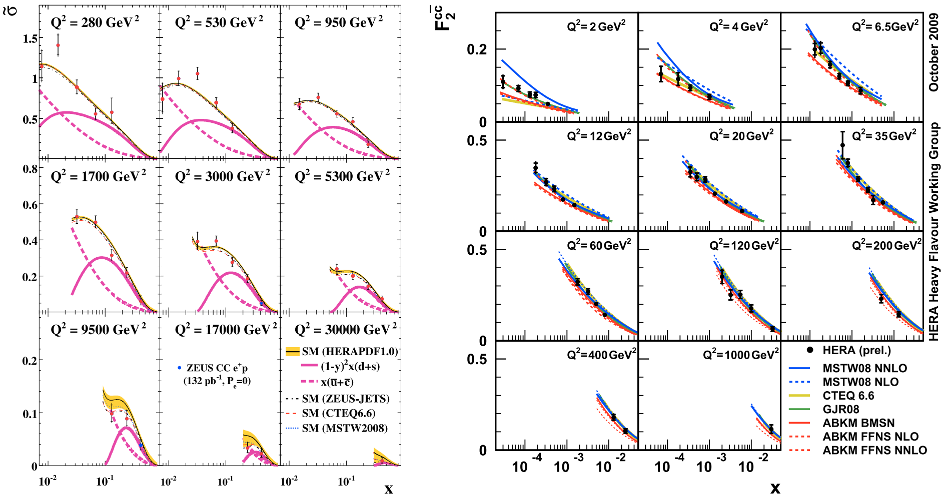


Figure 6: Access to the charm content of the proton. Left: through CC interactions, right: through D meson production.

While the CC data give a hint of charm, the production of D mesons in all varieties give a direct handle on the $c$ content. This is used to extract the charm structure functions. A preliminary result obtained from combined ZEUS and H1 data is depicted in Fig. 6(right). The charm structure function is an important input to LHC analyses, where the knowledge or lack thereof could provide a dominating systematic uncertainty.

recommended version →

| NAME | NC and CC DIS | NC, lower E(p_beam) | Jets | Charm | Docu | Grids | Data comparison | Date |
|---|---|---|---|---|---|---|---|---|
| HERAPDF1.7 NLO | HERAI + partial HERAII | H1+ZEUS | H1 and ZEUS(1) | H1+ZEUS | Figures | N.A. | | June 2011 |
| HERAPDF1.6 NLO | HERAI + partial HERAII | --- | H1 and ZEUS(1) | --- | Writeup and figures | N.A. | | March 2011 |
| HERAPDF 1.5 NNLO | HERAI + partial HERAII | --- | --- | --- | Figures | LHAPDF beta 5.8.6 | | March 2011 |
| HERAPDF 1.5 NLO | HERAI + partial HERAII | --- | --- | --- | Figures | LHAPDF beta 5.8.6 | | July 2010 |
| Charm mass scan | HERAI | --- | --- | H1+ZEUS | Writeup and figures | --- | | August 2010 |
| HERAPDF1.0 NNLO | HERAI | --- | --- | --- | ICHEP2010 writeup and figures | Docu for LHAPDF | | April 2010 |
| | HERAI | H1+ZEUS | --- | --- | Writeup and figures | N.A. | | April 2010 |
| | HERAI | --- | --- | H1+ZEUS | DIS2010 writeup and figures | N.A. | | April 2010 |
| HERAPDF1.0 NLO PUBLISHED | HERAI | --- | --- | --- | Paper HERAPDF1.0 page | LHAPDF | Benchmarking HERAPDF1.0 | Nov. 2009 |

Figure 7: Available HERAPDFs as seen on the web [4].

## 2.6 The HERAPDF family

The HERA data was used over the past years to create a family of PDFs. Data were included as results became available. The table depicted in Fig. 7 provides an overview as given on

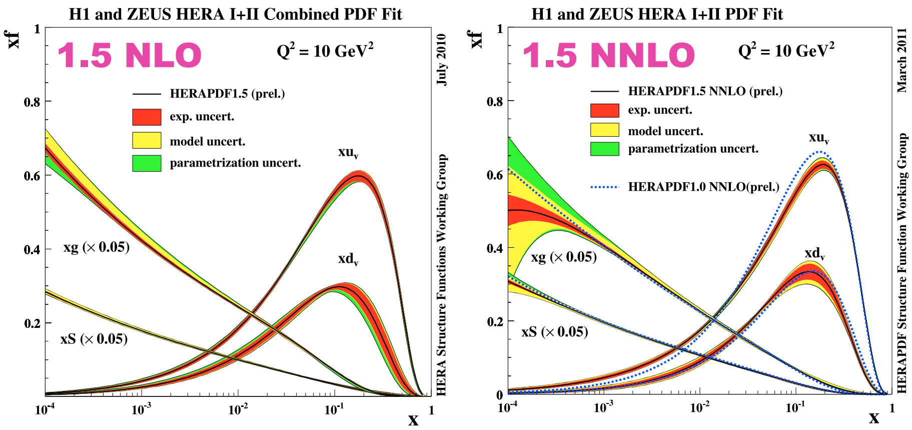


Figure 8: The currently recommended member of the HERAPDF family. The NNLO extraction has a larger uncertainty on the glue and the sea. Experimental, model and parametrisation uncertainties are given separately.

the net at the time of the conference [4]. The youngest member of the family, HERAPDF1.7, is not only based on inclusive measurements, but also on jet and charm data. Charm data was already used previously for a charm mass scan. The currently recommended version is HERAPDF1.5, available at next to leading order, NLO, and at next-to-next to leading order, NNLO, see Fig. 8. It is, as HERAPDF1.0, based on inclusive data only. As soon as the final results for the inclusive measurement of ZEUS and H1 as well as combination paper on charm will be published, a new major version of HERAPDF will be extracted.

The working group extracting, i.e. fitting, all the HERAPDFs has developed a tool named HERAfitter [5]. This tool allows the extraction of PDFs for a flexible set of input assumptions and input data. This tool has become "open source software" and is a service to the HEP community at large. It is not only used in the HERA, but also the LHC community.

# 3 HERAPDF goes LHC

The HERAPDFs are being used to predict the outcome of measurements done at the LHC. Figure 9 gives an example from CMS who measured the muon charge asymmetry from W decays. This is sensitive to the difference between the $u$ and $d$ valence quark distributions. HERAPDF1.5 is quite successful predicting this asymmetry.

LHC has also started to contribute to the PDFs. The HERAfitter tool was used to extract the strange quark content of the proton [6]. The strange quark cannot be well constrained by HERA data, as it would require a CC analysis of D mesons which so far is a "mission impossible".

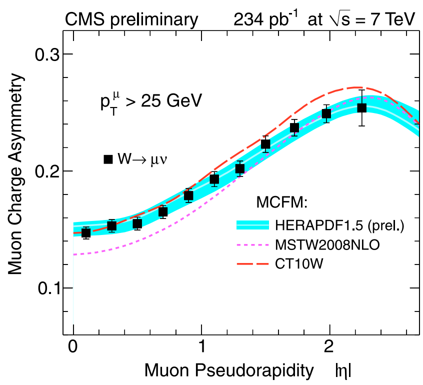


Figure 9: Muon charge asymmetry from $W$ decays compared to predictions.

## 4 Low-$x$ partons

The physical interpretation of PDFs is not clear to
the author. The parametrisations are not predicted by any theory; they are based on common sense arguments like they should be zero at $x = 1$. The variable $x$ itself is generally interpreted as the fraction of the momentum of the proton that a parton carries. At very low $x$, however, the Heisenberg uncertainty principle teaches us that such a parton cannot be confined inside a proton. The interpretation is only valid in a reference frame in which the proton is fast and in the context of a scattering process with a certain momentum transfer, $Q^2$. In the reference frame where the proton is at rest, the variable $x$ can be interpreted as $x \approx 0.1 \cdot l[\mathrm{fm}]$, where $l$ is the coherence length of fluctuations of the exchanged photon. For $x < 0.1$, $l$ is larger than the size of the proton of about 1 fm. A detailed discussion can be found in [7]. The effect is demonstrated in Fig. 10. The photon fluctuates into a quark-antiquark pair and this fluctuates further into a hadron like object which interacts with the proton.

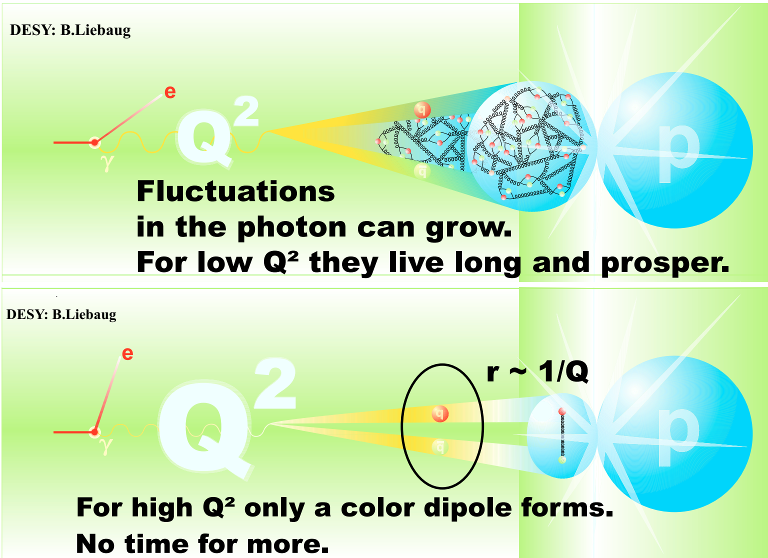


Figure 10: The *ep* scattering process in the rest frame of the proton. The photon looks like an extended object. At low $Q^2$ , top, it has time to grow into a complicated object. At high $Q^2$, bottom, there is only time to form a so called "color dipole".

In general, physics should not be dependent on the rest frame in which it is looked at. Therefore, the two different interpretations should only be seen as something to guide us through perturbation theory. Somehow, what me measure has to be connected to the structure of the underlying interaction. At low x, the PDFs represent more the strong and electroweak field than the proton. It would be nice to base the parametrisations that we use on some understanding of these fields. Another interesting question in this context is, whether the PDFs that could be measured in neutrino proton scattering would be the same as in electron proton scattering. After all, there is no photon to fluctuate in this case. The guess of the author is that at low $x$ the result would be different. The photon probably just looks like a hadron. Thus, probing with a hadron would give the same results as probing with a photon(electron).

# 5 Test of the color dipole picture

At the very end of the HERA running, data were taken at lower proton energies. This facilitated direct measurements of the longitudinal structure function $F_L$ [8, 9]. These measurement are tricky, because they require the identification of electrons with a relatively low energy, down to 3.4(6.0) GeV for H1(ZEUS). Both collaborations published results which clearly show that $F_L > 0$. The results on $F_L$ can be taken as a probe of higher orders of perturbative QCD, but they can also be used to test the color dipole picture[10]. The H1 collaboration compared their results to different model predictions as depicted in Fig. 11. The predictions based on the color dipole model deviate from the PDF-based ones at low $Q^2$. The data seem to have a preference to fall between the two ways of looking at things. It should be noted that nature does seem to have a sense of humor.

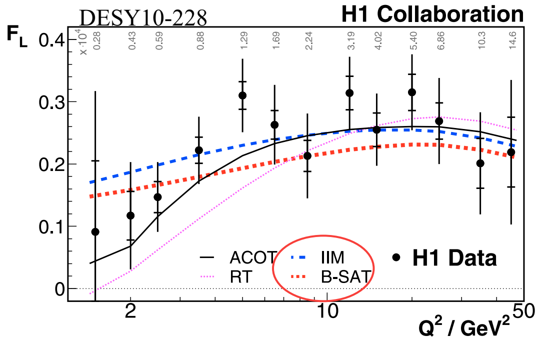


Figure 11: Measurement of the structure function $F_L$ compared to predictions from colour dipole models, IIM and B-SAT, and others, ACOT and RT [8].

Another test of the color dipole model is provided by Deeply Virtual Compton Scattering, DVCS. The measured dependence of the cross section on the squared momentum transfer at the proton vertex, t, was compared to predictions of the colour dipole model and the model did quite well [11].

# 6 The looks of a proton

The PDFs as so far discussed in this contribution only give information about what happens in momentum space. It is possible to define generalised parton distribution functions which are used for two-gluon exchanges like in DVCS. The interpretation then is in longitudinal momentum and transverse position space. The aforementioned dependence of the DVCS cross section on $t$ can be parametrised as $d\sigma/dt \sim exp(-b|t|)$ and $b$ can be converted to an average impact parameter. The H1 collaboration has done so [11] and obtained 0.65±0.02 fm for x=0.0012. Is this the transverse expansion of the partons engaged in the interaction? Is this the size of the proton? Or the size of the photon fluctuation? Or the relevant size of the field? Anyhow, there is a quite a number of b-slope measurements available, not only for DVCS, but also for vector meson production. It might be interesting to interpret these measurements with respect to impact parameters.

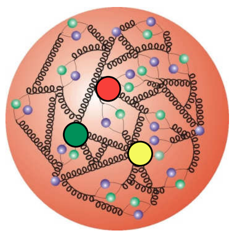

Figure 12: Standard illustration of a "HEP-proton". Three valance quarks are imbedded in a cocoon of gluons and sea quarks.

Most of the time, the "HEP-proton" is depicted as in Fig.12. The charge radius of the proton is not measured in HEP, high energy physics, but in low energy physics. The most precise values come from electronic and muonic hydrogen [12]. The rms values are 0.8768±0.0069 fm and 0.84184±0.00067 fm. The two values disagree by four standard deviations which in itself has triggered some discussion, including discussions about physics beyond the standard model. However, the value of 0.65 fm is certainly quite different. But that is something that should not surprise too much. The author would assume that the charge radius as measured at low energies is related to the valence quarks. The "radius" measured with DVCS is connected to x=0.0012 and that should not be valence quarks at all.

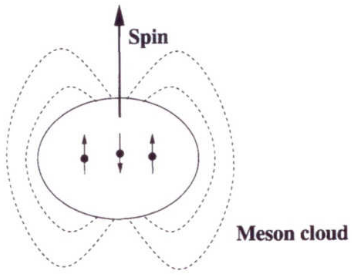


Figure 13: A proton as seen by a nuclear physicist [15]. It has a shape to support its magnetic moment and a meson cloud.

The picture of Fig.12 is in many ways misleading. Three charged objects as depicted would create an electric dipole moment, but this is known to be less than 0.54 $10^{-23}$ ecm. And in addition, the proton cannot be spherical at all, because it has a magnetic moment, which was first measured in proton → Δ excitations [13]; the most precise measurements come from single trapped protons [14]. The nuclear physicist's view of a proton is shown in Fig.13 [15]. Also shown is an indication of a meson cloud. This has to be there; otherwise the proton could not stick together with other baryons. This is again a completely different interpretation than typical HEP view of perturbative QCD. However, the meson cloud was observed in HEP, remember the EMC effect.

The next step in understanding the proton, or perhaps baryon or even nuclei in general, would be to match the pictures of nuclear physics with the ideas of QCD. There is some input on this from lattice QCD where the shape of baryons is actually predicted [16]. Figure 14 gives as an example the shape that is the result of a lattice QCD calculation.

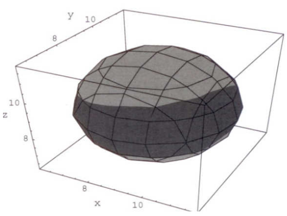

Figure 14: The shape of a Δ as predicted by lattice QCD [16].

It seems a worthwhile enterprise to think about ways how to measure such a shape and how to measure the spatial distribution of what is inside. In Fig. 1 it is shown, how we destroy the castle in order to find out what is inside and who just got married. It would be nice to open the door, have a look inside and just ask. However, many of the dynamics inside the castle might evade our observation, if we look with too much energy, because that means averaging over time; Heisenberg all over again.

# 7 Summary and Outlook

The proton as we know it still holds a lot of secrets. What is called the proton parton distribution functions, PDFs, was measured with excellent precision at HERA. The final results from HERA will be a very valuable legacy for a long time. They are expected within a year.

These PDFs are and will be one of the inputs to make precise Standard Model predictions for the LHC and other future experiments. The extraction of PDFs is one of the great success stories of HERA. The tools developed in this context will also survive and become part of the

HEP daily work.

The interpretation of proton PDFs in the context of understanding the proton itself is not trivial and there is more to the proton than PDFs. There are many questions about size, shape and the spatial distribution of quarks and gluons that should be addressed. In the end, it will take more than perturbative QCD to understand the proton.

# References


[1] H1 and ZEUS Collab., F.D. Aaron *et al.*, JHEP **01** (2010) 109.

[2] ZEUS Collab., S. Chekanov *et al.*, Eur.Phys.J. **C61** (2009) 223.

[3] ZEUS Collab., H. Abramowicz *et al.*, Eur.Phys.J. **C70** (2010) 945.

[4] `https://www.desy.de/h1zeus/combined_results/herapdftable`

[5] `http://herafitter.hepforge.org/`

[6] ATLAS Collab., "Determination of the strange quark density of the proton from ATLAS measurements of the $W \to l\nu$ and $Z \to ll$ cross sections", 2012. `hep-ex/1203.4051`

[7] A. Caldwell and G. Grindhammer, Physik Journal **6** (2007) 39.

[8] H1 Collab., F.D. Aaron *et al.*, Eur.Phys.J. **C71** (2011) 1579.

[9] ZEUS Collab., S. Chekanov *et al.*, Phys.Lett. **B682** (2009) 8.

[10] C. Ewerz *et al.*, "The New $F_l$ measurement from HERA and the Dipole model", 2012. `hep-ph/1206.6296`

[11] H1 Collab., F.D. Aaron *et al.*, Phys.Lett. **B659** (2008) 796.

[12] M. O. Distler *et al.*, Phys.Lett. **B696** (2011) 343.

[13] R. Beck *et al.*, Phys.Rev.Lett **78** (1997) 606.

[14] J. DiScaccia and G. Gabrielse, "Direct Measurement of the Proton Magnetic Moment", 2012. `hep-ph/1201.3038`

[15] A. Faessler, Progress in Particle and Nuclear Physics **44** (2000) 197.

[16] C. N. Papanicolas, Eur.Phys.J. **A18** (2003) 141.